POLITECNICO DI TORINO
Repository ISTITUZIONALE

Damage Localization in Framed Structures using Peridynamic Models

Original
Damage Localization in Framed Structures using Peridynamic Models / Crocetti, A., Betti, R., Ceravolo, R., Miraglia, G.. - In: THE E-JOURNAL OF NONDESTRUCTIVE TESTING. - ISSN 1435-4934. - ELETTRONICO. - 31:(2026), pp. 1-9. (12th European Workshop on Structural Health Monitoring (EWSHM 2026) Toulouse (France) July 7-10, 2026) [10.58286/33766].

Availability:
This version is available at: 11583/3014557 since: 2026-08-17T10:23:15Z

Publisher:
NDT.net

Published
DOI:10.58286/33766

Terms of use:

This article is made available under terms and conditions as specified in the corresponding bibliographic description in the repository

Publisher copyright

(Article begins on next page)

18 November 2026

More info about this article: https://www.ndt.net/?id=33766

Damage Localization in Framed Structures using Peridynamic Models

Alessio CROCETTI[1,2], Raimondo BETTI[3], Rosario CERAVOLO[1,2], Gaetano MIRAGLIA[1,2]

[1]Department of Structural, Geotechnical and Building Engineering, DISEG, Politecnico di Torino, Corso Duca degli Abruzzi 24, 10129 Turin, Italy, alessio.crocetti@polito.it, rosario.ceravolo@polito.it, gaetano.miraglia@polito.it
[2]Responsible Risk Resilience interdepartmental Centre, R3C, Politecnico di Torino, Corso Duca degli Abruzzi 24, 10129 Turin, Italy, alessio.crocetti@polito.it, rosario.ceravolo@polito.it, gaetano.miraglia@polito.it
[3]Department of Civil Engineering and Engineering Mechanics, CEEM, Columbia University, New York, NY 10027, USA, rb68@columbia.edu

Abstract This study investigates a novel technique to estimate new local vibration parameters to monitor existing buildings in the structural health monitoring field. The paper also gives a comprehensive discussion on their use for damage localization, as well as how these parameters are related to the variations of structural eigen-properties, with the aim of connecting local with global damage features. In order to estimate these new local vibrational parameters, the authors propose the implementation of a new modeling strategy based on peridynamics, which represents a novel continuum theory. This is performed under operational conditions assumptions, i.e., without the need to force the system with external inputs. The idea is to exploit the discrete formulation of peridynamics to build low-fidelity structural models, useful for rapid and scalable analyses. The focus of this study is to generate a network of points and bonds, where each point represents the spatial position of a significant location within a structure. The goal is to construct a bond force network that structurally connects these points, approximating the structural topology and connectivity of the system. Starting from the spatial coordinates of these points, the authors apply the peridynamic theory to determine the corresponding values of mass, stiffness, and damping parameters. This allows to build a simplified yet physically meaningful model of the structure, suitable for structural health monitoring. Within this framework, two parameters are obtained to localize damage: Bond Extremity Acceleration (BEA) and Bond Extremity Velocity (BEV). Both are derived from a micro-viscoelastic formulation of peridynamic bonds and can be indirectly estimated from acceleration response data using established techniques. The methodology is tested on a numerical reproduction of a three-story aluminum frame, modeled with 36 degrees of freedom and subjected to Gaussian noise. The conclusions of the study suggest that low-fidelity peridynamic models can be a useful basis for developing physical representations of structural networks, suitable for monitoring existing buildings and infrastructures.

Keywords: Structural Health Monitoring; Peridynamics; Damage Localization; Framed Structures; Low Fidelity Structural Models

Introduction

Reliable information on the health state of real structures can only be obtained within manageable computational times by balancing simulator accuracy and computational efficiency. To achieve this trade-off, a joint use of low- and high-fidelity models is useful, as low-fidelity approaches provide fast and scalable estimates while high-fidelity models deliver detailed

This work is licensed under CCBY 4.0

Media and Publishing Partner NDT.net
https://doi.org/10.58286/33766

and accurate predictions of complex structural responses. When Structural Health Monitoring (SHM) [1] is applied to a large number of structures (e.g., at the urban scale), very high-fidelity models often become impractical to provide information within feasible computational times. Peridynamics (PD) is a modern nonlocal continuum theory introduced in the early 2000s by Stewart Silling [2], further developed by Silling et al. [3], and it has recently attracted increasing attention in computational mechanics. In the literature, PD applications span several research fields [4], including particle systems, biology, and multiscale modeling. Although PD has been widely investigated for damage and fracture simulation, its adoption as a modeling paradigm within SHM is still relatively modest. In particular, the estimation and identification of PD model parameters for damage detection, aimed at SHM applications in the built environment, remains largely unaddressed. In this context, it is worth noting that, while PD-based SHM contributions are limited, system identification techniques following classical continuum mechanics are well established and widely used in practice [5]. System identification is particularly valuable for damage definition [6], where damage is commonly defined as a change in the system that negatively affects its current or future performance [7]. Accordingly, SHM seeks to define damage indices (either physically interpretable or purely data-driven) that are applicable to both linear and nonlinear systems. Within this perspective, equations of motion derived from a specific peridynamic formulation, namely Bond-Based Peridynamics (BBPD) [2], provide a basis for introducing monitoring statistics with a direct physical interpretation. In PD, the governing integral equations relate the internal material state (e.g., internal force field) to measurable structural responses (e.g., displacements). Building on this concept, two PD-based SHM features were proposed in [8]: the Bond Extremity Acceleration (BEA) and the Bond Extremity Velocity (BEV). When PD is used for SHM of existing structures, the discretization is often constrained by sensor placement and practical experimental requirements. From a monitoring standpoint, BEA can be interpreted as a "virtual" acceleration associated with the bond restoring action and is therefore expected to decrease as damage reduces bond stiffness. BEV is defined analogously and is proportional to BEA through a bond-level damping parameter.

The paper proposes a peridynamic modeling strategy to support scalable SHM analyses. In particular, a BBPD formulation is used to define local monitoring features at the bond level, focusing on the BEA due to its higher reliability to model-structure discrepancies [8]. The main contributions of this work are stated: (i) the construction of a low-fidelity peridynamic network model of a three-story framed structure; (ii) the computation of bond-level features, namely BEA, under a systematic set of bond damage scenarios and severity levels; (iii) the development and validation of two fully connected neural classifiers for damage localization (Net 1) and joint localization and severity assessment (Net 2), including validation analyses under increasing feature noise; and (iv) a numerical testing phase in which BEA is estimated from acceleration responses and then the networks are tested on Stochastic Subspace Identification (SSI) identified features. The remainder of the paper is organized as follows. Section 1 introduces the BBPD formulation and the proposed identification procedure. Section 2 reports the numerical case study and discusses the results for damage localization and severity assessment. Finally, Section 3 summarizes the main conclusions.

1. Methods

1.1 Bond-based Peridynamics

The PD theory relies on the force-interactions of points, called *bonds*. The bond-based PD theory (BBPD) [2] is a special case of PD where force density vectors are equal in magnitude and parallel to the corresponding position vector in the deformed state, resulting in pairwise

This work is licensed under CCBY 4.0

Media and Publishing Partner NDTnet

interactions of material points. Modeling can be pursued according to the PD theory by subdividing the matter into infinitesimal portions, described by their mass and volume. Every point k is then able to interact with a limited number of neighbors inside a region. The family of k is defined as the collection of all the points inside the region. The extent of the latter is characterized by the *horizon*, which represents the maximum distance over which point k can interact with other points in the body. This parameter represents the locality of the behavior of the system and it can be constant or variable along the space or, in some cases, can be defined based on calibration procedures [9]. Choosing a small horizon results in a more local behavior. In particular, the classical theory of elasticity can be seen as a limiting case of BBPD for which the horizon approaches zero [10]. Starting from the nonlinear micro-viscoelastic bond formulation [2], and after expressing the bond stretch and its rate in terms of the relative displacement field, the linearized micro-linear viscoelastic BBPD equation of motion [11] can be stated as

$$\mathbf{M}\,\ddot{\mathbf{u}}(t) + \mathbf{C}\,\dot{\mathbf{u}}(t) + \mathbf{K}\,\mathbf{u}(t) = \mathbf{z}(t) \tag{1}$$

$$\mathbf{M} = \begin{bmatrix} \mathbf{M}_k & \mathbf{O}_3 & \cdots \\ \mathbf{O}_3 & \ddots & \cdots \\ \vdots & \vdots & \ddots \end{bmatrix} \; ; \; \mathbf{C} = \begin{bmatrix} \sum_{\substack{j=1 \\ j\neq k}}^{K} \mathbf{C}_{kj} & -\mathbf{C}_{kj} & \cdots \\ -\mathbf{C}_{kj} & \ddots & \cdots \\ \vdots & \vdots & \ddots \end{bmatrix} \; ; \; \mathbf{K} = \begin{bmatrix} \sum_{\substack{j=1 \\ j\neq k}}^{K} \mathbf{K}_{kj} & -\mathbf{K}_{kj} & \cdots \\ -\mathbf{K}_{kj} & \ddots & \cdots \\ \vdots & \vdots & \ddots \end{bmatrix} \tag{2}$$

$$\begin{aligned} \mathbf{M}_k &= m_k \mathbf{I}_3, \\ \mathbf{C}_{kj} &= \nu_{kj}\,\mathbf{K}_{kj}, \\ \mathbf{K}_{kj} &= c_{kj}\,V_k V_j\,\boldsymbol{\Xi}_{kj} \\ \boldsymbol{\Xi}_{kj} &= \frac{\boldsymbol{\xi}_{kj}\,\boldsymbol{\xi}_{kj}^{\mathsf{T}}}{\|\boldsymbol{\xi}_{kj}\|^3} \\ c_{kj} &= \begin{cases} c_{kj}, & \|\boldsymbol{\xi}_{kj}\| \le h, \\ 0, & \|\boldsymbol{\xi}_{kj}\| > h, \end{cases} \\ \boldsymbol{\xi}_{kj} &= \mathbf{x}_j - \mathbf{x}_k. \end{aligned} \tag{3}$$

In Eqs. (1) and (3), the position of point k is stated in the vector $\mathbf{x}_k = (x_{k,X}, x_{k,Y}, x_{k,Z})^{\mathsf{T}}$ (and analogously for point j). The vector $\boldsymbol{\xi}_{kj} = \mathbf{x}_j - \mathbf{x}_k$ describes the bond connecting the two points, whose interaction is restricted to the horizon h. The terms V_k and V_j correspond to the nodal volumes associated with points k and j. The parameter $c_{kj} \geq 0$ is the bond (linear elastic) constant, whereas $\nu_{kj} \geq 0$ is a bond damping constant. Moreover, m_k is the mass lumped at point k, $\mathbf{I}_3$ is the 3×3 identity matrix and $\mathbf{O}_3$ indicates the 3×3 zero matrix.

1.2 Parameters identification

At this point, two different parameters can be derived and used as features for structural health monitoring; the Bond Extremity Acceleration (BEA) $w_{kj}^{'}$, and the Bond Extremity Velocity (BEV) $w_{kj}^{''}$, of the bond kj and the extremity k.

$$w_{kj}^{'} = \frac{c_{kj}\,V_j V_k}{m_k} \tag{4}$$

$$w_{kj}^{''} = w_{kj}^{'}\,\nu_{kj} \tag{5}$$

This work is licensed under CCBY 4.0

Media and Publishing Partner NDTnet

It is important to state that in Eqs. (4) and (5), in the general case, $w'_{kj} \neq w'_{jk}$ and $w''_{kj} \neq w''_{jk}$ as $m_k \neq m_j$. These parameters are useful because they can be easily identified experimentally without the need for input sources (i.e. operational conditions). Once the acquired acceleration response $\ddot{\mathbf{u}}(t)$ is obtained, it is therefore possible to get an estimate of the system matrix $\hat{\mathbf{A}}$ in the state space formulation, limited to the measured DoFs. This can be estimated, for instance, using Stochastic Subspace Identification (SSI) algorithms [12]. By performing the eigenanalysis of $\hat{\mathbf{A}}$, after some manipulations, it is possible to obtain the real eigenvalue matrix $\mathbf{\Lambda}$ of the reduced system (squared natural circular frequencies), the real eigenvectors $\mathbf{\Phi}$ and the damping ratios $\mathbf{Z}$. In detail, both $\mathbf{\Lambda}$ and $\mathbf{Z}$ are diagonal matrices containing the sorted eigenvalues and the damping ratios, respectively, while $\mathbf{\Phi}$ includes the associated eigenvectors in each column of the matrix.

$$\hat{\mathbf{A}} = \begin{bmatrix} \mathbf{O} & \mathbf{I} \\ -\hat{\mathbf{M}}^{-1}\hat{\mathbf{K}} & -\hat{\mathbf{M}}^{-1}\hat{\mathbf{C}} \end{bmatrix} \tag{6}$$

Since the reliability of the BEV parameter strongly depends on model–structure discrepancies, this makes it less suitable for a confident use in SHM applications [8]. Focusing, instead, in the determination of the BEA matrix, and writing the undamped case, the modal equilibrium equation of the reduced system reads

$$\hat{\mathbf{K}}\mathbf{\Phi} = \hat{\mathbf{M}}\mathbf{\Phi}\mathbf{\Lambda}. \tag{7}$$

By left-multiplying both sides by $\hat{\mathbf{M}}^{-1}$, it is possible to obtain

$$\hat{\mathbf{M}}^{-1}\hat{\mathbf{K}}\mathbf{\Phi} = \mathbf{\Phi}\mathbf{\Lambda}. \tag{8}$$

So, the quantity $\hat{\mathbf{M}}^{-1}\hat{\mathbf{K}}$ required to compute the BEA can be identified directly from the estimated modal parameters, $\mathbf{\Phi}$ and $\mathbf{\Lambda}$, by minimizing the Frobenius norm of the residual from the eigen equation:

$$\min_{\hat{\mathbf{M}}^{-1}\hat{\mathbf{K}}} \left\| \hat{\mathbf{M}}^{-1}\hat{\mathbf{K}}\mathbf{\Phi} - \mathbf{\Phi}\mathbf{\Lambda} \right\|_F^2. \tag{9}$$

It is important to note that the eigenvalue problem is implicitly affected by a scale indeterminacy, since a simultaneous scaling of $\hat{\mathbf{M}}$ and $\hat{\mathbf{K}}$ keeps the modal solution constant and insensitive to this change. In order to remove this issue, the lumped mass associated with the first DoF was fixed to a known reference value ($m_1 = 0.59$ kg), while the remaining parameters were estimated through nonlinear least-squares minimization of the modal residual. Once $\hat{\mathbf{M}}^{-1}\hat{\mathbf{K}}$ is obtained, the BEA matrix $\hat{\mathbf{W}}'$ can be computed by performing an element-wise operation with the geometric micro-modulus matrix $\mathbf{\Delta}$ (Hadamard operator $\circ$):

$$\hat{\mathbf{W}}' = \left[-\hat{\mathbf{M}}^{-1}\hat{\mathbf{K}} \right] \circ \mathbf{\Delta}^{\circ -1}, \tag{10}$$

$$\mathbf{\Delta} = \begin{bmatrix} \mathbf{I}_3 & \mathbf{\Xi}_{kj} & \cdots \\ \mathbf{\Xi}_{kj} & \ddots & \cdots \\ \vdots & \vdots & \ddots \end{bmatrix}. \tag{11}$$

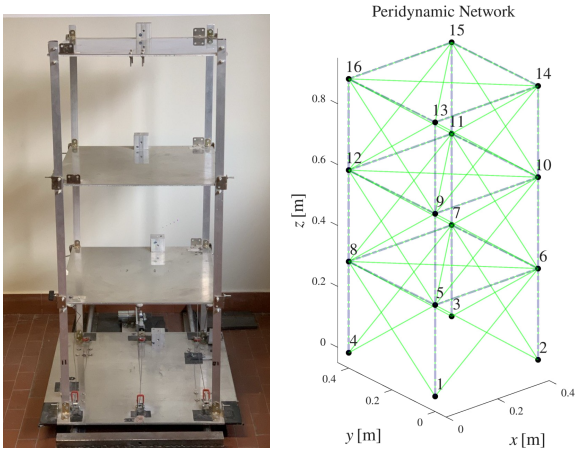
2. Results and discussion

2.1 Peridynamic Network

The proposed methodology has been validated with a numerical model of the three-story aluminum frame (Fig. 1a) located at the Earthquake Engineering and Dynamics (EED) Laboratory; further details are reported in [13, 14]. The frame has a total height of 0.9 m and a square plan with side length $L = 0.4$ m. The peridynamic network was modeled by considering the frame joints as points (Fig. 1b). The horizon was set equal to $h = \sqrt{2}L$, corresponding to the in-plane diagonal distance between opposite points. Based on this discretization, the point masses and associated volumes were defined, and a nominal value of the bond elastic constant c_{kj} was assigned according to the equation:

$$c_{kj} = \chi \frac{E_{kj}}{h} \tag{12}$$

where $\chi = 6.25$ is a corrective factor in order to ensure consistency with the physical properties of the frame and $E_{kj} = 6.9 \times 10^{10}$ Pa is the Young's modulus. Stochastic variability was introduced through Gaussian noise to account for material dispersion and parameter uncertainties. After assembling the global matrices, the DoFs associated with the fixed-base nodes (i.e., the first four column nodes) were constrained, leading to the reduced system matrices **M**, **C**, and **K** consistent with the imposed boundary conditions and the remaining free DoFs. An eigenvalue analysis was then performed to extract the first two natural frequencies (f_1, f_2), adopting a mode-tracking procedure to associate the correct mode. Subsequently, damage scenarios were applied. For each bond, a progressive reduction of the nominal bond elastic constant c_{kj} was imposed in 10% increments, up to a maximum reduction of 90%, in order to simulate increasing damage severity levels. For each value of c_{kj}, 9000 samples were generated to obtain statistical distributions of the BEA parameters (and natural frequencies under both undamaged and damaged conditions, having 1000 samples for each severity level). For each configuration, BEA values (w'_{kj}) and natural frequencies were extracted accordingly. A total of 54 distinct bonds were damaged, resulting in 486 damage cases.



(a) (b)

Fig. 1. *(a) Reference three-story aluminum frame benchmark; (b) corresponding peridynamic network.*

2.2 Model development and validation for damage localization and severity assessment

A dataset including the first two natural frequencies (f_1, f_2) and the BEA parameters (w'_{kj}), for both undamaged and damaged configurations of each bond, was used to train and validate

two different classifiers: (i) a damage localization model, hereinafter referred to as Net 1 (i.e., identification of the damaged bond), and (ii) a damage localization and severity assessment model, denoted as Net 2 (i.e., identification of both the damaged bond and its severity level). Both classifiers consist of fully connected neural networks using LeakyReLU activation functions and dropout regularization, and were trained using the Adam optimizer. The validation metrics for Net 1 and Net 2 are reported in Table 1.

2.2.1 Corrupted dataset

The robustness of the networks was assessed by introducing noisy input data. For each bond reduction, corresponding to a given damage severity class, the standard deviation of the features was computed. The noise level was then scaled consistently with the statistical dispersion of the data, by applying a predefined error grid to both the natural frequencies and the BEA parameters (Fig. 2). Accordingly, for each noise level, a perturbed dataset was generated by corrupting the original features with Gaussian noise. The resulting performance of the networks under increasing noise levels is reported in Fig. 3a and Fig. 3b.

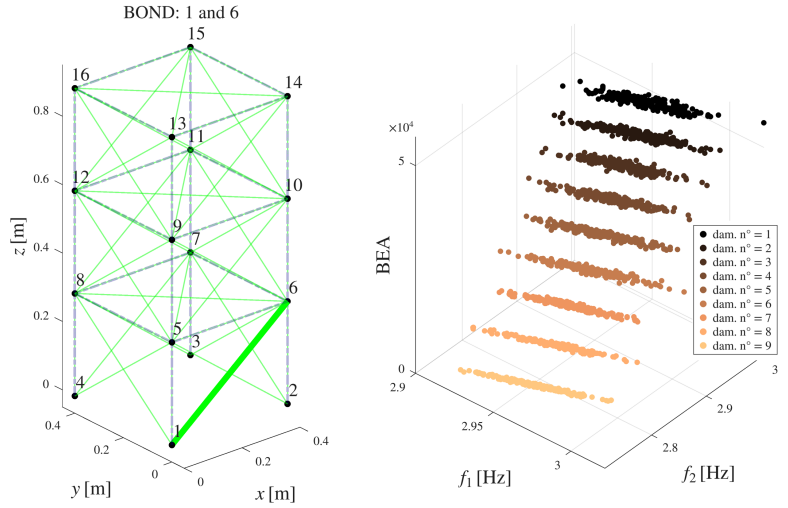
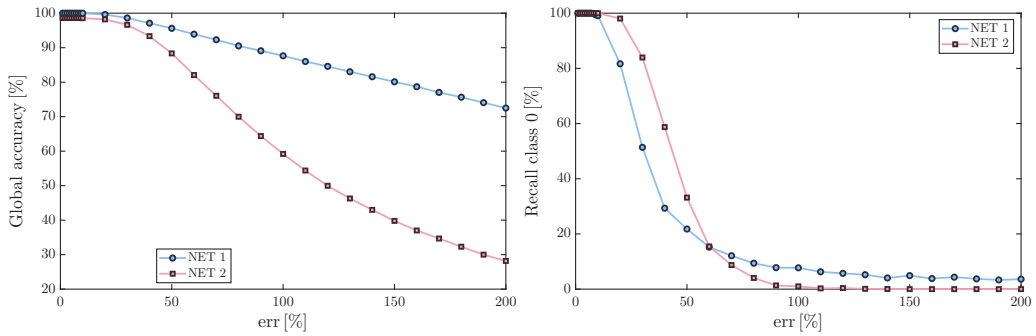


Fig. 2. *Comparison of noise-corrupted BEA and natural frequencies across damage severity levels for a representative damaged bond.*



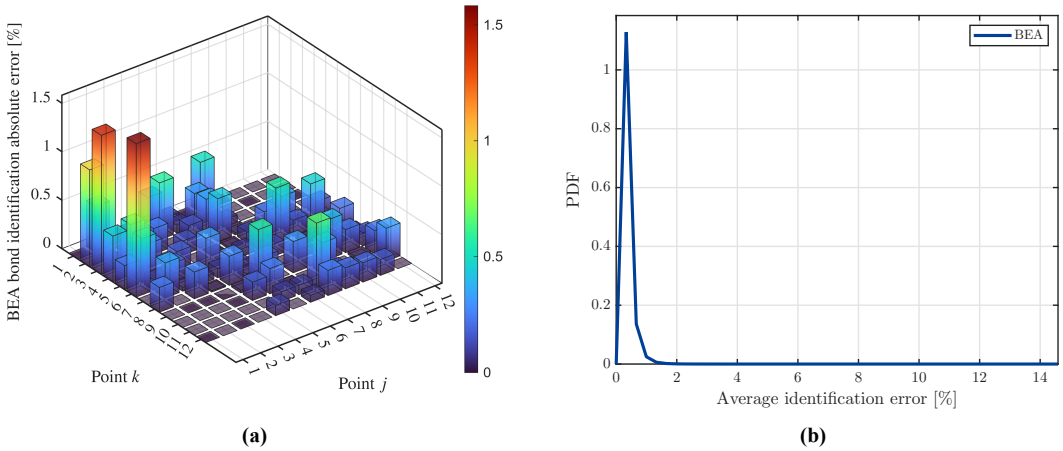
(a) **(b)**

Fig. 3. *Classifier performance under increasing feature noise: (a) global accuracy for Net 1 and Net 2; (b) recall of the undamaged class (Class 0) for Net 1 and Net 2.*

2.2.2 System identification results

To test the classifiers, the dynamic response under ambient excitation was simulated and system identification was performed using SSI [12] on 5 independent acquisitions per structural

condition, consisting of 210 minutes simulated signals corrupted with 5% Gaussian noise. From the identified state-space models, the natural frequencies and the BEA parameters were estimated. To ensure the identification of all relevant modes of the system, the sampling frequency was set to 350 Hz. Fig. 4 reports the bond absolute identification error in the undamaged configuration, defined as the absolute difference between the target and the identified BEA values, normalized with respect to the target value, for each bond. The BEA parameters were estimated according to Eq. 10. The performance obtained by testing the networks on the identified data is summarized in Table 1, while the confusion matrix for Net 1 is reported in Fig. 5. It is worth noting that data associated with labels 2–13 are not included, since the BEA parameters corresponding to the degrees of freedom constrained at the fixed supports cannot be identified due to the reduced system matrices **M** and **K**.



(a) **(b)**

Fig. 4. *Identification performance at 5% noise. (a) Bond absolute error; (b) PDF of the identification error.*

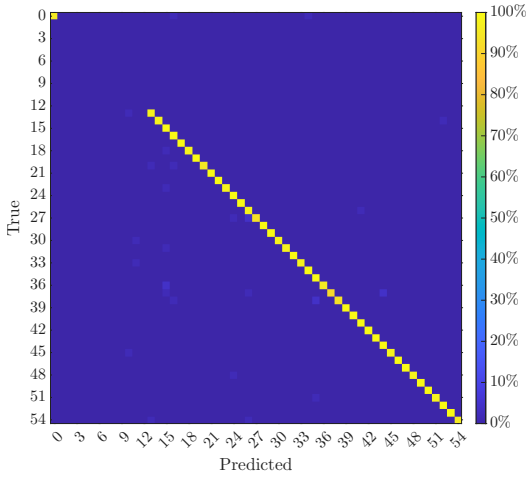


Fig. 5. *Confusion matrix of Net 1 tested on SSI-identified features. Class 0 represents the undamaged condition, whereas the remaining classes correspond to damaged-bond cases (labels associated with constrained DoFs are excluded).*

Table 1. Performance metrics for Net 1 and Net 2.

Net	Phase	Accuracy	Macro F1	Damage accuracy	Precision Cl.0	Recall Cl.0
1	Validation	100.00%	100.00%	100.00%	100.00%	100.00%
1	Test SSI	98.50%	98.61%	98.57%	100.00%	95.56%
2	Validation	98.63%	98.41%	98.60%	100.00%	100.00%
2	Test SSI	78.45%	74.89%	78.04%	100.00%	95.56%

This work is licensed under CCBY 4.0

Media and Publishing Partner NDTnet

3. Conclusions

This paper proposes a bond-based PD framework to estimate novel vibration-based parameters for structural health monitoring. Using the discrete PD formulation, a low-fidelity structural model of a three-story aluminum frame was developed. A bond force network was then constructed to emulate the structural connectivity and provide a meaningful representation of the system. Within this framework, the Bond Extremity Acceleration (BEA) parameter was computed under multiple damage scenarios and used to develop two classifiers: (i) a damage-localization model to identify the damaged bond (Net 1), and (ii) a model to estimate both the damaged bond and its severity level (Net 2). In detail:

- A total of 54 bond damage cases were considered over 9 severity levels, resulting in 486 damaged configurations (in addition to the undamaged case). Two different classifiers were then trained and validated (Net 1 and Net 2).
- The classifiers were tested under increasing Gaussian noise on the input features; BEA remained stable with noise amplification, providing high global accuracy.
- BEA was indirectly estimated from acceleration responses via SSI under operational conditions. Testing was then performed on the identified features, reaching a global accuracy of 98.50% for Net 1 and 78.45% for Net 2.

The results indicate that BEA is a scalable and physically interpretable parameter for damage monitoring in structural networks. While the numerical findings are promising, experimental validation is required to confirm the reliability of the approach under real operating conditions.

4. Acknowledgments

This publication is part of the project PNRR-NGEU which has received funding from the MUR – DM 118/2023.

References

[1] Farrar, C. R. and Worden, K. “An Introduction to Structural Health Monitoring”. In: *New Trends in Vibration Based Structural Health Monitoring*. Ed. by Maier, G., Rammerstorfer, F. G., Salençon, J., Schrefler, B., Serafini, P., Deraemaeker, A., and Worden, K. Vol. 520. Series Title: CISM International Centre for Mechanical Sciences. Vienna: Springer Vienna, 2010, pp. 1–17. DOI: 10.1007/978-3-7091-0399-9_1.

[2] Silling, S. A. “Reformulation of elasticity theory for discontinuities and long-range forces”. en. In: *Journal of the Mechanics and Physics of Solids* 48.1 2000, pp. 175–209. DOI: 10.1016/S0022-5096(99)00029-0.

[3] Silling, S. A., Epton, M., Weckner, O., Xu, J., and Askari, E. “Peridynamic States and Constitutive Modeling”. en. In: *Journal of Elasticity* 88.2 2007, pp. 151–184. DOI: 10.1007/s10659-007-9125-1.

[4] Javili, A., Morasata, R., Oterkus, E., and Oterkus, S. “Peridynamics review”. en. In: *Mathematics and Mechanics of Solids* 24.11 2019, pp. 3714–3739. DOI: 10.1177/1081286518803411.

[5] Ljung, L. “System Identification”. en. In: *Wiley Encyclopedia of Electrical and Electronics Engineering*. Ed. by Webster, J. G. 1st ed. Wiley, 1999. DOI: 10.1002/047134608X.W1046.

[6] Wang, Z., Lin, R., and Lim, M. “Structural damage detection using measured FRF data”. en. In: *Computer Methods in Applied Mechanics and Engineering* 147.1-2 1997, pp. 187–197. DOI: 10.1016/S0045-7825(97)00013-3.

[7] Farrar, C. R. and Worden, K. *Structural Health Monitoring: A Machine Learning Perspective*. en. 1st ed. Wiley, 2012. DOI: 10.1002/9781118443118.

This work is licensed under CCBY 4.0

Media and Publishing Partner

[8] Miraglia, G., Lenticchia, E., Civera, M., and Ceravolo, R. "Assessing Structural Health State by Monitoring Peridynamics Parameters in Operational Conditions". en. In: *Experimental Vibration Analysis for Civil Engineering Structures*. Ed. by Wu, Z., Nagayama, T., Dang, J., and Astroza, R. Vol. 224. Series Title: Lecture Notes in Civil Engineering. Cham: Springer International Publishing, 2023, pp. 39–50. DOI: 10.1007/978-3-030-93236-7_5.

[9] Bobaru, F., Foster, J. T., Geubelle, P. H., and Silling, S. A., eds. *Handbook of Peridynamic Modeling*. en. 0th ed. Chapman and Hall/CRC, 2016. DOI: 10.1201/9781315373331.

[10] Madenci, E. and Oterkus, E. *Peridynamic Theory and Its Applications*. en. New York, NY: Springer New York, 2014. DOI: 10.1007/978-1-4614-8465-3.

[11] Silling, S. A. "Linearized Theory of Peridynamic States". en. In: *Journal of Elasticity* 99.1 2010, pp. 85–111. DOI: 10.1007/s10659-009-9234-0.

[12] Van Overschee, P. and De Moor, B. *Subspace Identification for Linear Systems*. en. Boston, MA: Springer US, 1996. DOI: 10.1007/978-1-4613-0465-4.

[13] Dragonetti, P., Civera, M., Miraglia, G., and Ceravolo, R. "A Benchmark Dataset for the Validation of Phase-Based Motion Magnification-Based Experimental Modal Analysis". en. In: *Data* 10.4 2025, p. 45. DOI: 10.3390/data10040045.

[14] Crocetti, A., Miraglia, G., and Ceravolo, R. "Using Similarity Distance Measures for Multiclass Damage Detection in Dynamically Monitored Structures". en. In: *Structural Control and Health Monitoring* 2025.1 2025. Ed. by Li, J., p. 9593577. DOI: 10.1155/stc/9593577.

This work is licensed under CCBY 4.0

Media and Publishing Partner NDT.net